

RESEARCH

Open Access



# Effect of Contents, Tensile Strengths and Aspect Ratios of Hooked-End Steel Fibers (SFs) on Compressive and Flexural Performance of Normal Strength Concrete

Seok-Joon Jang<sup>1</sup>, Wan-Shin Park<sup>2</sup>, Sun-Woo Kim<sup>2</sup>, Dong-Hui Kim<sup>3</sup>, Qi Wang<sup>3</sup>, Woo-Jin Jeong<sup>3</sup>, Ai-Hua Jin<sup>3</sup> and Hyun-Do Yun<sup>3\*</sup>

## Abstract

This study is a part of the study to simplify the reinforcing details of reinforced concrete (RC) structural members by substituting the conventional reinforcement with hooked-end steel fibers (SFs). This paper investigates the effects of SF strength, dosage and aspect ( $l/d$ ) ratio on the compressive and flexural behaviors of normal strength concrete with specified compressive strength of 30 MPa. In this study, hooked-end SFs of high strength (2000–2400 MPa) and normal strength (1100–1200 MPa) were used with three  $l/d$  ratios of 64, 67 and 80. Hooked-end SFs were incorporated with three dosages of 20 kg/m<sup>3</sup> (0.25 vol.%), 40 kg/m<sup>3</sup> (0.50 vol.%) and 60 kg/m<sup>3</sup> (0.75 vol.%). Eighteen steel fiber reinforced concrete (SFRC) mixes were mixed. To evaluate the compressive and flexural performance of each SFRC mixture, three SFRC cylindrical and prismatic specimens for each mixture were manufactured and tested, respectively. The test results that the inclusion of hooked-end SFs had little effect on the compressive strength, while it improved the toughness of concrete. Hooked-end SFs were also found to be effective in enhancing the flexural performance of concrete. The dosage and properties (strength and  $l/d$  ratio) of SFs significantly affect the residual flexural tensile strength ( $f_{R1}$  and  $f_{R3}$ ) at serviceability (SLS) and ultimate limit state (ULS) defined in fib Model Code 2010 (MC2010).

**Keywords** Steel fiber reinforced concrete (SFRC), Compressive behavior, Flexural behavior, Toughness, Residual flexural strength

## 1 Introduction

Concrete has become the most popularly used construction material for civil infrastructures over the worldwide due to its easy material supply, simple manufacturing process, low cost, superior compressive strength and durability. However, plain concrete has inherent drawbacks such as low tensile strength and brittle behavior. The addition of SFs into concrete matrix has been recognized as an effective methodology to improve the tensile strength and the post-cracking behavior of plain concrete (Pakravan et al., 2017; Wang et al., 2021).

The first scientific research on the use of SFs on concrete was conducted in the 1960s (Romualdi & Batson, 1963). During the early 1960s, the studies were

Journal information: ISSN 1976-0485 / eISSN 2234-1315

\*Correspondence:

Hyun-Do Yun  
wiseroad@cnu.ac.kr

<sup>1</sup> Building Management Support Center, Korea Authority of Land & Infrastructure, Jinju 52856, Republic of Korea

<sup>2</sup> Department of Construction Engineering Education, Chungnam National University, Daejeon 34134, Republic of Korea

<sup>3</sup> Department of Architectural Engineering, Chungnam National University, Daejeon 34134, Republic of Korea

concentrated on the evaluation of the potential for SFs to control concrete cracks. In addition, the influence of adding SFs on the properties of freshly mixed steel fiber reinforced concrete (SFRC) was investigated (Balaguru & Ramakrishnan, 1988; Johnston, 1984). The tendency of a SFRC mixture to produce fiber balling in the freshly mixed state was found to be a function of the maximum size and the particle size distribution of aggregate, the method of adding SFs into the concrete mixture, and properties, such as the  $l/d$  ratio, the volume fraction and the shape, of SFs.

Since 1970s, numerous studies have been performed to investigate the SFs reinforcing effects on the hardened properties of plain concrete. From these works, it is known that discrete, short and randomly distributed SFs in hardened concrete is effective to control crack's width due to the ability of SFs to transfer the developed tensile stresses across a cracked section called as crack-bridging after cracking. In market, various shapes of SFs were supplied as a reinforcement for concrete. It has been reported that the hooked-end SFs are very effective for improving the post-cracking properties of concrete due to the higher bond strength and superior stress transmission between cement matrix and hooked-end SFs. The incorporation of hooked-end SFs into concrete resulted in improving the flexural and shear strength (Abbass et al., 2018; Shoaib & Lubell, 2021), energy absorption capacity (ACI Committee 544, 2009; Zollo, 1997), shrinkage resistance (Li et al., 2020), permeability (Marcos-Meson et al., 2018), spalling and impact resistance (Soufeiani et al., 2016; Zhang et al., 2020). Despite better mechanical properties of SFRC evinced in these many studies, the SFs was limitedly used for thermal and shrinkage cracking control in the concrete members and the structural contribution of SFs was not considered due to the lack of international codes and design guidelines for the structural design of SFRC members.

In particular, the favorable characteristics of SFRC under tension, i.e., improved residual strength and ductility, showed the feasibility of using short hooked-end SFs as a promising reinforcement which can fully or partially replace the conventional reinforcement in concrete elements. Mertol et al. (2015) investigated the effect of hooked-end SFs' addition on the flexural behavior of reinforced concrete beams with different longitudinal reinforcement ratios. The test results indicated that the incorporation of SFs increased the strength, stiffness and ductility of reinforced concrete beams with longitudinal reinforcement ratio of less than 1.5%, while for over-reinforced sections, it is not clear to improve the flexural performance by adding SFs. Kytinou et al., 2020 investigated analytically the contributions of SFs on the initial stiffness, flexural strength, deformation capacity, cracking

behavior, and residual stress of RC beams through the 3D finite element analysis (FEA) model, which was verified with a test database of 17 large-scale reinforced SFRC beams collected from the literature.

Recently, (Shoaib & Lubell, 2021) proposed the relationship between the compressive, flexural and direct shear responses for SFRC containing hooked-end SFs with yield strength of 1100 MPa and  $l/d$  ratio of 55 at 0 to 1% by volume for use in member-scale structural design. Choi et al., 2019 proposed a probabilistic analysis technique using SDEM (Simplified Diversity Embedment Model) to evaluate the multiple cracking mechanism of high-performance fiber-reinforced concrete (HPFRC). The analysis results showed that the actual strain-hardening tensile behavior of HPFRC specimens can be reasonably predicted by the number of segments selected based on fiber length. Bhogone & Subramaniam, 2021 reported that steel fibers provide the highest  $\sigma$  as a function of  $w$  compared to polypropylene fibers. The difference in the  $\sigma$ - $w$  response between polypropylene and steel fiber-reinforced concrete increases with age, while the energy of failure increases steadily with age. The improvement of the post-cracking behavior of steel fibers over time is due to the increased resistance to crack propagation and fiber pull-out. The blend of micro and macro polypropylene fibers shows higher resistance to crack propagation and fiber pull-out compared to macro polypropylene fibers alone. The torsional behavior and analysis of steel fiber reinforced concrete (SFRC) beams were examined by Deifalla et al., 2021. The comparison of predicted strengths to experimental values from performed torsion tests indicated potential for improvement. The application of the proposed model showed greater compliance and consistency with experimental results compared to available design models that provide validated and safe predictions. Gao & Wang, 2021 investigated the effects of recycled fine aggregate and SFs with yield strength of 1160 MPa and  $l/d$  ratio of 65 on the compressive and splitting tensile properties of high strength concrete. Guler & Akbulut, 2022 evaluated the mass loss, compressive and flexural strength, and toughness capacities of normal strength SFs with modified end geometries. Chen et al., 2022 examined the effects of novel multiple hooked-end SFs on the flexural tensile behavior of notched high-strength concrete beams by BS EN 14651. Therefore, it is thought that conventional reinforcement might be partially replaced with SFs as structural reinforcement to prevent the brittle failure of critical structural members in the civil infrastructure.

Over the last decades, the utilization of SFs as partial or total replacement material of traditional reinforcement bars or meshes in the structural elements has been recognized as a popular solution to reduce the construction

period and to control the width of thermal or shrinkage cracks (ACI committee 544, 2009; Serna et al., 2009; The Concrete Society, 2007). The SFs are being applied to various types of concrete, such as cast-in-place concrete, precast concrete, and shotcrete. Through the research, development and application spanning more than 50 years, the national codes covering the design of SFRC elements have been established (ACI Committee 318, 2008; fib Bulletin 65/66: Model Code 2010, 2012). The shear capacity of SFRC elements with no shear reinforcement was reviewed by Lantsoght (Lantsoght, 2019), who pointed out the shortcomings in our understanding of the shear behavior of such elements and proposed the necessary steps to address these shortcomings. Using experimental data, Kytinou et al., 2020 proposes a model that incorporates nonlinearities of the materials, including constitutive relationships for SFRC under compression and tension. A new smeared crack approach for the tensional response of SFRC is proposed, which uses stress versus crack width relations with tension softening instead of stress–strain laws. The study extensively compares numerical and experimental results, demonstrating that the model accurately captures key aspects of the response, such as SFRC tension softening, tension stiffening, bending moment–curvature envelope, and the beneficial effect of steel fibers on the residual response. The efficiency of steel fibers as a replacement for minimum conventional steel stirrups in RCA-based deep beams with web openings was investigated by Kachouh et al., 2022. It was found that the use of 1% steel fiber volume fraction in the RCA-based beam with openings without steel stirrups was sufficient to restore 96% of the original shear capacity of the NA-based beam with conventional steel stirrups. The effectiveness of a wireless SHM system in detecting damage caused by cracking was investigated in FRC with synthetic fibers under compressive repeated load in Voutetaki et al., 2022's study. The study found that the measurements of the PZT transducers were influenced by distance-, direction-, and damage-level triggers, and the RMSD index was found to be a reliable statistical tool for assessing structural damage.

Early design provisions were prescribed by (ACI Committee 318, 2008) which introduced the use of SFs with reference to minimum shear reinforcement. The fib Model Code (MC2010) (fib Bulletin 65/66: Model Code 2010, 2012) provides the design methodology for the bending, axial compression, shear and torsion of reinforced SFRC members. In both codes, the design of SFRC and the introduction of its properties in structural calculations are based on the pre- and post-crack flexural response from SFRC standard beam tests. It is commonly known that the flexural performance of SFRC depends on concrete strength, fiber volume fraction and

the properties, such as the geometry, tensile strength and  $l/d$  ratio, of SFs (ACI Committee 544, 2009); Serna et al., 2009; The Concrete Society, 2007). Similar to this approach, for hybrid fiber-reinforced cement composites, Abadel et al., 2016 and Almusallam et al., 2016 developed the fiber reinforcing index as a parameter to characterize the mechanical properties, taking into consideration the effect of fibers, similar to FRC. The fiber reinforcing index is calculated based on variables, such as fiber strength, content, and aspect ratio, and research (Li et al., 2018) has also been conducted to investigate the relationship between the mechanical properties of hybrid fiber-reinforced cement composites and this index. In particular, fiber dosage is the most effective factor in the flexural tensile behavior of SFRC. The flexural toughness and flexural residual strength of SFRC can be improved by increasing the amount of SF addition (Abbass et al., 2018; Choi et al., 2019). However, it is very important to have the homogeneous distribution and random orientation of SFs and to prevent the segregation or balling of SFs during mixing. To obtain the superior flexural residual strength of SFRC, the amount of SF addition should be increased. Higher content of SFs alters the rheology of the concrete and gives rise to an apparent loss of consistence (ACI Committee 544, 2009); Serna et al., 2009; The Concrete Society, 2007). The workability of SFRC is recognized as one of the major obstacles in applying SFRC to structural members. Therefore, it is required to provide a methodology for improving the structural performance of the SFRC, especially the flexural residual strength, within the range that does not impair the manufacturing and construction performance of the SFRC.

As an effective alternative to improving the flexural performance without degrading the workability of SFRC, the addition of high strength steel fibers into concrete may be considered. Although extensive research is being conducted on SFRC, the effects of high tensile strengths of hooked-end SF with various  $l/d$  ratios and contents on the flexural performance of normal concrete have been rarely reported in the available literature. In the study by Chen et al., 2021, the tensile strength of steel fibers was used as an experimental variable, but since the length, diameter, aspect ratio, and hook shape of steel fibers differ, it is not possible to quantitatively evaluate the effect of the tensile strength of steel fibers on the flexural behavior of FRC.

The purpose of this study is to address the limitations of previous research on SFRC by evaluating the influence of various steel fiber parameters on the compressive and flexural performance of concrete with an uncompressed strength of 30 MPa. Specifically, this study focuses on the impact of parameters, such as the  $l/d$  ratio, which is known to vary greatly depending on the type of steel

fiber, and particularly the tensile strength of the steel fibers, on the compressive and flexural performance of concrete. By providing a quantitative evaluation of the impact of these parameters on the compressive and flexural behaviors of SFRC, this study offers valuable insights into the design and optimization of SFRC. In addition, the results of this study have the potential to provide information for the development of international standards and guidelines for SFRC, thereby advancing the state of practice and promoting the widespread adoption of SFRC in civil engineering applications.

## 2 Experimental Investigation

The experimental investigation was programmed to investigate the compressive and flexural performance of SFRC using hooked-end SFs. The test variables designed in the study consist of fiber type (tensile strength and *l/d* ratio) and fiber dosage. In evaluating compressive performance of SFRC, the test variables effect on the compressive strength, stress–strain curve, Poisson’s ratio and toughness of SFRC was examined. To investigate the SF properties effect on the flexural performance, the load–crack mouth opening displacement (CMOD), failure mode, flexural residual strength and fracture energy were examined.

## 2.1 Materials and Mixture Proportion

All the SFRC and control concrete mixtures were prepared using ordinary Portland cement (Type I) from a local cement plant. Locally available crush natural limestone with particle sizes between 5 and 20 mm was used as coarse aggregates. Crushed sand with the fineness modulus of 2.92 was used for the preparation of mixes. Six different hooked-end SFs were used to produce the SFRC. The physical properties and configurations of the hooked-end SFs are provided in Table 1. The identifier of SFs represents the strength and *l/d* ratio of SFs. For instance, NSF64 and HSF64 indicate the normal strength and high strength SFs with *l/d* ratio of 64, respectively.

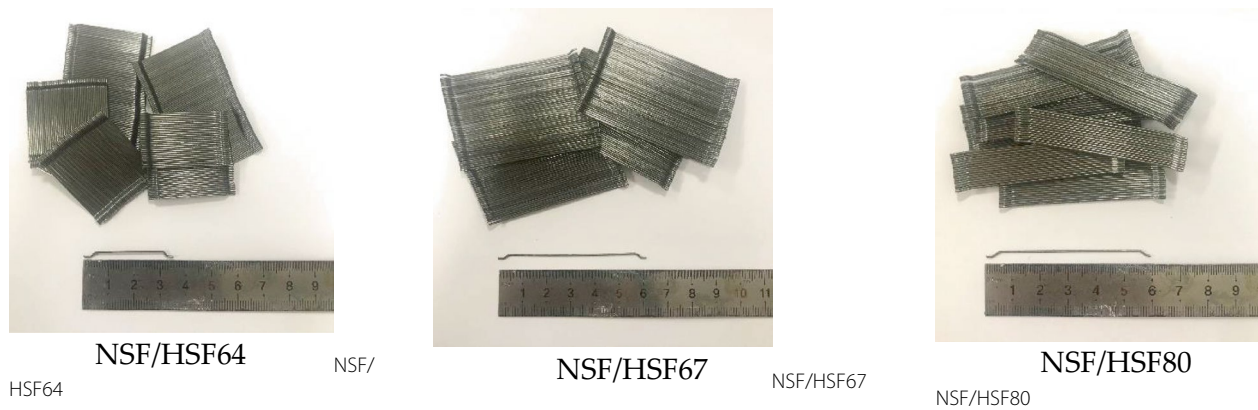
The proportion and description of control concrete mixture is summarized in Table 2. Control concrete mixture is a target 28-day compressive strength of 30 MPa. Water to cement (W/C) ratio is 0.55. To produce SFRCs, six types of SFs with different tensile strength and aspect ratio were used. Three different dosages of the SFs were added to the concrete mixture at 20 kg/m<sup>3</sup> (0.25 vol.%), 40 kg/m<sup>3</sup> (0.50 vol.%) and 60 kg/m<sup>3</sup> (0.75 vol.%). The

**Table 2** Mixture design proportion of concrete

Mixture	W/C (%)	Water (kg/m <sup>3</sup> )	Cement (kg/m <sup>3</sup> )	Sand (kg/m <sup>3</sup> )	Aggregate (kg/m <sup>3</sup> )
Concrete	55	129	235	557	669

**Table 1** Properties and configurations of hooked-end SFs

Designation	Length (mm)	Diameter (mm)	Aspect ratio ( <i>l/d</i> )	Tensile strength (MPa)
NSF64	35	0.55	64	1100
NSF67	60	0.90	67	1200
NSF80	60	0.75	80	1100
HSF64	35	0.55	64	2000
HSF67	60	0.90	67	2400
HSF80	60	0.75	80	2100



designation of SFRC mixture is denominated in the combination types and dosages of SFs. For instance, NSF64-20 refers to the SFRC mixture reinforced with NSF64 steel fibers at the dosage of 20 kg/m<sup>3</sup>.

### 2.2 Specimen Preparation

A single batch was used for manufacturing all specimens in the given designation of concrete and SFRC. Concrete was prepared in 100 L horizontal shaft mixer. First, dry components, such as cement, sand and aggregate, were mixed for 1 min. Then, water and the polycarboxylate superplasticizer were added into the dry mixture and mixed again for 3 min. The mixer was stopped and the control concrete mixture was cast in different molds to manufacture three cylindrical and three prismatic specimens. For preparing SFRC specimens, SFs were dispersed manually into the fresh concrete mixture after the preparation of concrete mixture in the mixer and mixed well for 5 min.

For each SFRC mix, three cylindrical specimens of 150×300 mm were prepared to evaluate the compressive performance of SFRC. Three prismatic specimens of 150×150×550 mm were cast for the flexural strength test in the rigid steel molds. The flexural specimens were cast according to the procedure of filling the mold in EN 12350-1 EN 12350-1, (2009). All specimens were covered with plastic sheet to maintain moist conditions. The specimens were demolded after 24 h and stored under 100% relative humidity at the temperature of 22 ± 2 °C until the age of testing.

### 2.3 Testing Procedure

The concrete and SFRC cylindrical specimens for compressive strength were load-controlled and tested at the age of 28 days. A compressive testing machine with a capacity of 1000 kN was used to compress the concrete

and SFRC cylindrical specimens. To measure the longitudinal and transverse strain along the length of cylindrical specimens during compressive loading, two strain gauges for each direction were attached on the surface of cylinder. Two LVDTs were also mounted through compressometer to measure the displacement in the center gauge length of 150 mm of cylindrical specimen. According to Korean standard KS F 2405 (Korean standard, 2017), the loading rate for the compressive strength test was 0.6 MPa per second. Each result is the average strength of the three specimens.

The flexural pre- and post-cracking response of SFRCs was evaluated by means of monotonic three-point bending tests. According to BS EN 14651 (EN 14651, 2005), the test is performed on 150×150×550 mm SFRC beam with a span of 500 mm and a small notch of 25 mm depth at the midspan. A clip gauge was mounted along the longitudinal axis across the notch at the midspan to measure the CMOD, as shown in Fig. 1. The flexural loading rate was controlled using the CMOD and 0.2 mm per minute. Three prismatic specimens were tested for each SFRC mixture.

## 3 Results and Discussion

### 3.1 Compressive Behavior

The mean compressive strength results of three cylindrical specimens for all mixes are shown in Table 3. Table 3 presents the compressive strength, characteristic strength, secant modulus of elasticity, Poisson’s ratio, peak strain and compressive toughness. The elastic modulus, Poisson’s ratio, peak strain and compressive toughness were obtained from mean compressive strain based on the measurement of two strain gauges attached on the surface of specimens.

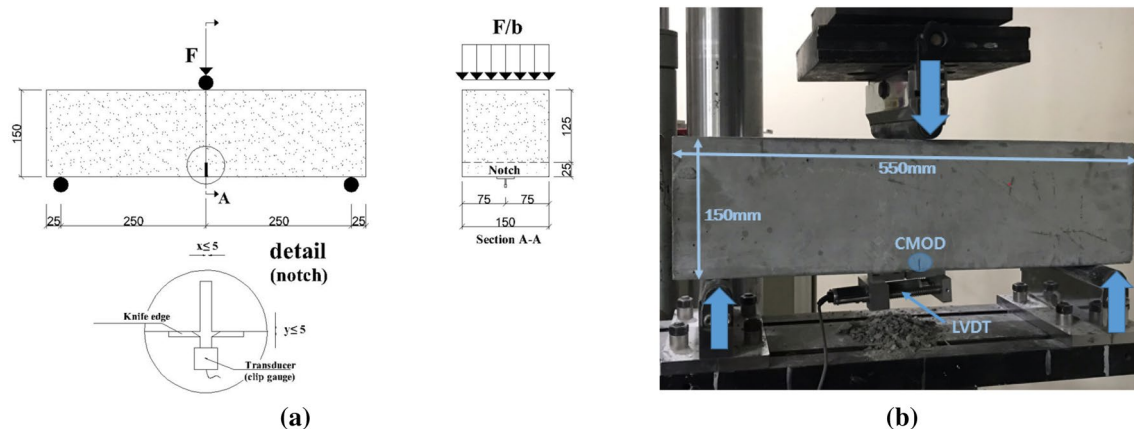


**Fig. 1** Flexural test setup **a** schematic representation (unit: mm) and **b** photo for setup

**Table 3** Test results on compressive properties of cylindrical specimens

Mixture	$f_{cm}$ ( $\sigma$ ) MPa	$f_{ck}$ MPa	$E_{cm}$ ( $\sigma$ ) GPa	$\epsilon_{co}$ ( $\sigma$ ) $10^{-6}$	$\nu$ ( $\sigma$ ) $10^{-2}$	$T_c$ ( $\sigma$ ) Joule
Concrete	24.1 ( $\pm$ 1.5)	21.6	27.3 ( $\pm$ 1.4)	1336.5( $\pm$ 133.7)	13 ( $\pm$ 1.0)	288.8 ( $\pm$ 69.2)
NSF64-20	22.3 ( $\pm$ 1.1)	20.5	25.0 ( $\pm$ 0.6)	1838.5( $\pm$ 134.1)	20 ( $\pm$ 1.0)	328.5 ( $\pm$ 25.0)
NSF64-40	22.7 ( $\pm$ 0.8)	21.4	22.9 ( $\pm$ 0.7)	1789.7( $\pm$ 115.5)	19 ( $\pm$ 1.0)	507.0 ( $\pm$ 36.7)
NSF64-60	24.2 ( $\pm$ 0.3)	23.7	22.7 ( $\pm$ 0.5)	2013.3( $\pm$ 132.9)	19 ( $\pm$ 0.0)	818.6 ( $\pm$ 36.2)
NSF67-20	24.5 ( $\pm$ 0.3)	24.0	27.4 ( $\pm$ 1.1)	1836.5( $\pm$ 14.8)	18 ( $\pm$ 1.0)	358.2 ( $\pm$ 49.7)
NSF67-40	23.9 ( $\pm$ 1.2)	21.9	26.8 ( $\pm$ 0.9)	1467.5( $\pm$ 121.1)	18 ( $\pm$ 1.0)	454.5 ( $\pm$ 46.6)
NSF67-60	24.8 ( $\pm$ 0.9)	23.3	26.9 ( $\pm$ 0.6)	1935.1( $\pm$ 25.2)	20 ( $\pm$ 2.0)	846.2 ( $\pm$ 28.0)
NSF80-20	21.7 ( $\pm$ 0.2)	21.4	25.6 ( $\pm$ 1.2)	1763.3( $\pm$ 48.9)	17 ( $\pm$ 2.0)	348.3 ( $\pm$ 10.6)
NSF80-40	21.5 ( $\pm$ 0.9)	20.0	22.3 ( $\pm$ 0.3)	2001.0( $\pm$ 204.3)	18 ( $\pm$ 2.0)	645.9 ( $\pm$ 82.6)
NSF80-60	22.9 ( $\pm$ 1.6)	20.3	22.2 ( $\pm$ 0.2)	1967.5( $\pm$ 129.4)	21 ( $\pm$ 4.0)	940.1 ( $\pm$ 53.4)
HSF64-20	24.3 ( $\pm$ 0.4)	23.6	31.6 ( $\pm$ 3.7)	1445.7( $\pm$ 229.3)	20 ( $\pm$ 2.0)	532.3 ( $\pm$ 69.9)
HSF64-40	21.8 ( $\pm$ 0.9)	20.3	27.3 ( $\pm$ 0.1)	1481.5( $\pm$ 489.7)	18 ( $\pm$ 1.0)	497.9 ( $\pm$ 173.3)
HSF64-60	24.5 ( $\pm$ 1.3)	22.4	27.5 ( $\pm$ 0.2)	1703.4( $\pm$ 210.1)	21 ( $\pm$ 2.0)	622.1 ( $\pm$ 6.9)
HSF67-20	25.1 ( $\pm$ 2.0)	21.8	28.2 ( $\pm$ 0.1)	1541.1( $\pm$ 263.7)	18 ( $\pm$ 3.0)	585.2 ( $\pm$ 132.5)
HSF67-40	27.3 ( $\pm$ 1.0)	25.7	28.0 ( $\pm$ 0.9)	1726.2( $\pm$ 107.5)	21 ( $\pm$ 1.0)	737.4 ( $\pm$ 114.8)
HSF67-60	30.2 ( $\pm$ 1.5)	27.7	26.9 ( $\pm$ 0.5)	1969.2( $\pm$ 141.8)	19 ( $\pm$ 1.0)	844.3 ( $\pm$ 22.5)
HSF80-20	23.0 ( $\pm$ 1.3)	20.9	27.7 ( $\pm$ 1.5)	1431.7( $\pm$ 262.1)	17 ( $\pm$ 0.0)	505.4 ( $\pm$ 107.1)
HSF80-40	24.6 ( $\pm$ 0.7)	23.4	30.0 ( $\pm$ 0.7)	1504.1( $\pm$ 133.4)	19 ( $\pm$ 1.0)	664.4 ( $\pm$ 29.0)
HSF80-60	24.9 ( $\pm$ 0.7)	23.7	27.8 ( $\pm$ 0.6)	1921.2( $\pm$ 255.3)	20 ( $\pm$ 2.0)	710.1 ( $\pm$ 102.4)

$f_{cm}$ : mean compressive strength;  $f_{ck}$ : characteristic compressive strength by MC2010;  $E_{cm}$ : mean secant modulus of elasticity;  $\epsilon_{co}$ : mena strain at compressive strength;  $\nu$ : mean Poisson's ratio;  $T_c$ : compressive toughness by JSCE-SF5 JSCE-SF5, 1984;  $\sigma$ : standard deviation

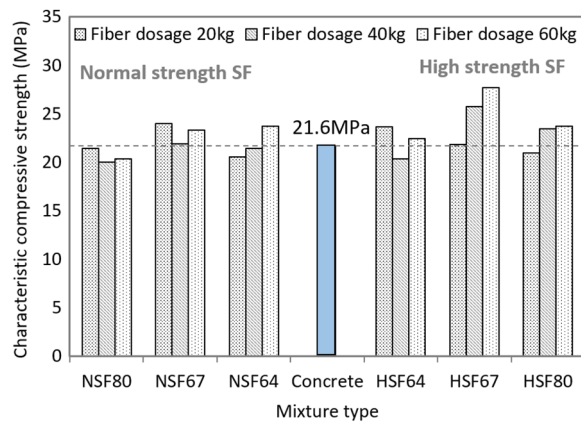


**Fig. 2** Characteristic compressive strength of SFRC cylinders

**3.1.1 SFs' Properties Influence on the Strength**

The compressive strength of control concrete and SFRC cylinders were measured after 28 days of water curing. As shown in Table 3, mean and characteristic compressive strength of conventional concrete at the age of 28 days were 24.1 and 21.6 MPa, respectively. The characteristic compressive strength is defined as the level of strength below which no more than 5% of the test result are expected to fall (fib Bulletin 65/66: Model Code 2010, 2012).

The maximum compressive strength was achieved in SFRC mixture with HSF67 SFs. The SFRC mixture with HSF67 SFs at the dosage of 20 kg/m<sup>3</sup>, 40 kg/m<sup>3</sup>, and 60 kg/m<sup>3</sup> had 0.9%, 19.0%, and 28.2% higher characteristic compressive strengths than that of conventional concrete, respectively. Fig. 2 shows that the characteristic compressive strength of SFRCs except for HSF67 mixture was not significantly affected by the addition of SFs up to a dosage of 60 kg/m<sup>3</sup> (0.75%) used in the investigation. However, it can be concluded that the usage of SFs with higher tensile strength and lower *l/d* ratio at the same SF content is advantageous for improving the compressive strength. Secant modulus of elasticity shows a similar trend of compressive strengths.

**3.1.2 SFs' Properties Influence on the Failure Patterns**

Typical compressive failure pattern of SFRC mixtures with different dosage and properties of hooked-end SFs is shown in Fig. 3. Concrete specimen failed due to vertical cracks induced by the tensile stress perpendicular to the loading direction and the wide spalling of concrete around the vertical cracks at its peak stress. Meanwhile, with adding SFs into concrete mixture up to 20 kg/m<sup>3</sup>, 40 kg/m<sup>3</sup>, and 60 kg/m<sup>3</sup>, the spalling of concrete in the SFRC specimens was remarkably reduced and diagonal cracks with angles of about 60° are shown due to the

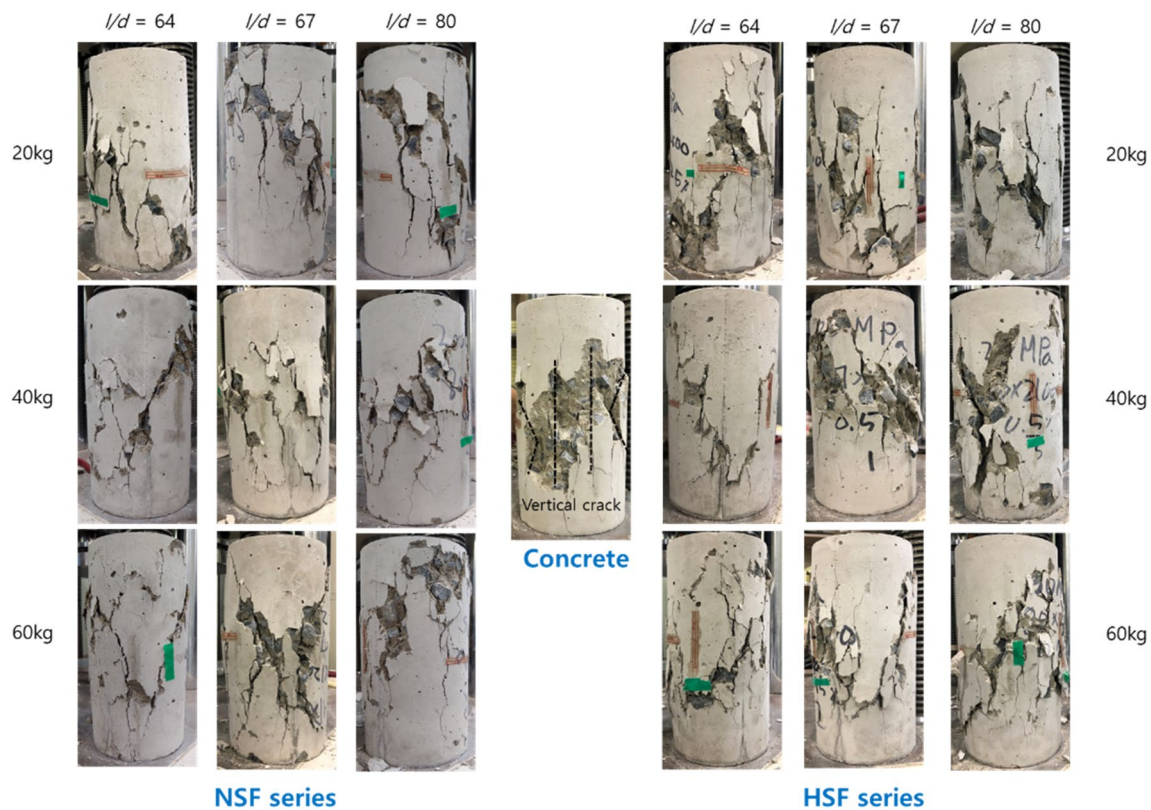


**Fig. 3** Typical failure pattern of SFRC cylinders in compression

shear mechanism of SFs. The widths of cracks in SFRC specimens is slightly smaller than that of conventional concrete. The failure of SFRC specimen is dominated by shear cracks. When the dosage of SFs was increased, SFRC specimens exhibited a failure pattern with multiple vertical or oblique cracks (Ding & Kusterle, 2000; Li et al., 2017; Yazıcı et al., 2007).

From Fig. 3, it can be seen that the failure pattern of SFRC specimen under compression is considerably affected by the added SF content. The SFs incorporated in the concrete matrix bridge cracks in the cement matrix and control the width of cracks after cracking. With increasing the SF content, SFRC cylinder in compression exhibits from brittle failure mode by several vertical cracks and wide spalling to ductile failure mode by multiple shear and vertical cracks. As shown in Fig. 3, the properties, such as tensile strength and  $l/d$  ratio, of SFs have little effect on the failure mode of SFRC cylinder in compression.

### 3.1.3 SFs' Properties Influence on Stress–Strain Response

Stress and strain curves of structural materials are not only regarded as one of the significant indexes to characterize the mechanical behavior, but also are required for modeling and analyzing structural members numerically.

Thus, the compressive stress and strain curves of SFRC specimens with different content and properties of SFs have been provided in this study.

Fig. 4 illustrates SF content and properties effect on typical stress and strain behavior of SFRC specimens. For each mixture, three specimens were tested and during compressive loading, axial strain was measured by two concrete gauges bonded at the center of cylinder. Strain in Fig. 4 is an average value of axial strains measured by two strain gauges. For all the SFRC mixtures, the shapes of stress and strain curves are similar.

In the ascending region which the stress increases with increasing strain, the curve shows initially linear elasticity and approaches to the peak stress. The stress–strain relationships showed no significant difference up to a point at approximately 70–80% of peak stress, where micro-crack begin to generate and propagate. Then, as the strain was increased, the stress and strain response showed a slight difference according to the dosage of SFs.

Compressive toughness ( $T_c$ ) is defined as the area below the stress and strain curve (JSCE-SF5, 1984). In this study, for the compressive toughness calculation based on JSCE-SF5, both the ascending curve in this compression experiment and the descending curve predicted using the formula proposed by Lee et al., (2015)

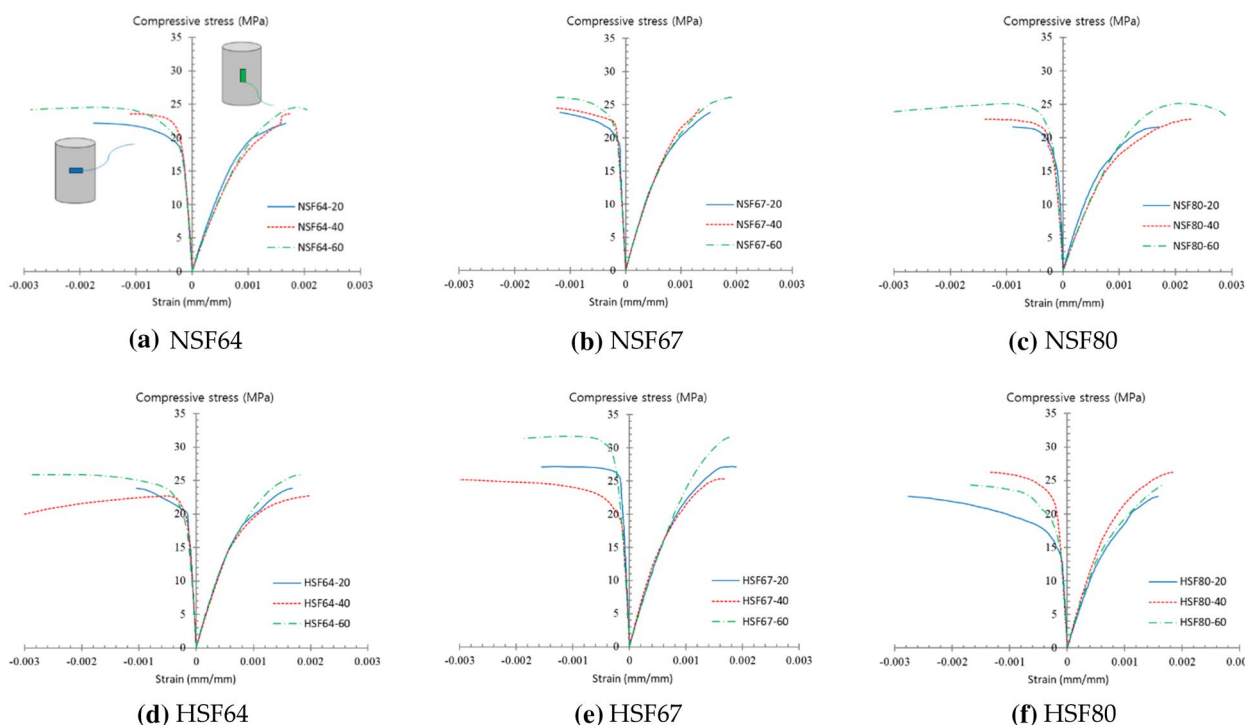


**Fig. 4** Typical stress–strain responses of SFRC cylinders in compression

were used. As shown in Table 3, compressive toughness increased as the dosage of SFs increased. The compressive toughens of SFRC incorporating high strength steel fiber was highest when the  $l/d$  ratio was 67. This increase in toughness is believed to be due to the increase in the bonding area, since the diameter of HSF67 is the largest at 0.90 mm. When the SFs dosage was low, the effect of steel fiber strength on compressive toughness was clearly evident. However, when the SFs dosage was 80 kg/m<sup>3</sup>, the influence of steel fiber strength was almost negligible. The elastic modulus showed a slight decrease as the dosage of SFs increased, while the influence of  $l/d$  ratio or tensile strength of SF was negligible.

### 3.2 Flexural Behavior

To investigate the influence of the dosage and properties of hooked-end SFs on the flexural performance of normal strength concrete, three notched SFRC beams for each SFRC mixture were manufactured and tested according to EN 12350–1 and EN 14651, respectively. The average flexural strength properties of the three prismatic specimens for all the concrete and SFRC mixes are shown in Table 4.

#### 3.2.1 SFs’ Properties Influence on the Failure Mechanism

The typical failure patterns of SFRC notched prismatic specimens under three-point bending were shown in Fig. 5. It is observed that the dosage and properties of SFs have positive effect on the failure behaviors of normal strength concrete with specified strength of 30 MPa.

For notched plain concrete specimens, the formation of the first crack started from the tip of the notch and the width of the crack increases as the CMOD increases. Upon failure, the crack extends to the top side of the cross section. The plain concrete specimens were fractured immediately after initial cracking and showed an obvious brittle failure mode.

Due to the fiber crack-bridging effect in SFRC specimens, the initial crack started from the tip of the notch propagated gradually upwards and changed its orientation as the bending load increases. Compared with plain concrete specimen, SFRC specimen showed multiple cracking behavior and effectively controlled the crack widths up to final failure.

As shown in Fig. 5, the length of main crack started from the tip of the notch decreases with the increase of SF dosage. In addition, higher  $l/d$  ratio and tensile strength of SFs are also effective to control the propagation of main crack. The main crack extends the middle height of the cross section in SFRC specimens mixed with NSF67-60, NSF80-60, HSF67-60 and HSF80-60,

**Table 4** Test results on flexural properties of prismatic specimens

Mixture	$f_L$ ( $\sigma$ ) MPa	$f_{R1}$ ( $\sigma$ ) MPa	$f_{R3}$ ( $\sigma$ ) MPa	$f_{LK}$ ( $\sigma$ ) MPa	$f_{R1K}$ MPa	$f_{R3K}$ MPa	$f_{R1K}/f_{LK}$	$f_{R3K}/f_{R1K}$ (class)	$G_F$ ( $\sigma$ ) $10^3 \times J/m^2$
Concrete	3.5 ( $\pm 0.1$ )	–	–	3.3	–	–	–	–	–
NSF64-20	3.8 ( $\pm 0.3$ )	1.8 ( $\pm 0.4$ )	2.1 ( $\pm 0.5$ )	3.3	1.1	1.3	0.33	1.18 (1.0c)	1.210 ( $\pm 0.279$ )
NSF64-40	4.4 ( $\pm 0.1$ )	2.8 ( $\pm 0.5$ )	4.1 ( $\pm 0.6$ )	4.2	2.0	3.1	0.47	1.55 (2.0e)	2.053 ( $\pm 0.328$ )
NSF64-60	4.6 ( $\pm 0.1$ )	3.3 ( $\pm 0.4$ )	4.8 ( $\pm 0.7$ )	4.4	2.6	3.6	0.59	1.38 (2.5e)	2.460 ( $\pm 0.331$ )
NSF67-20	3.6 ( $\pm 0.0$ )	1.4 ( $\pm 0.1$ )	1.9 ( $\pm 0.2$ )	3.6	1.2	1.6	0.33	1.33 (1.0e)	0.987 ( $\pm 0.008$ )
NSF67-40	4.8 ( $\pm 0.0$ )	3.4 ( $\pm 0.1$ )	3.9 ( $\pm 0.1$ )	4.8	3.2	3.7	0.66	1.15 (3.0d)	2.118 ( $\pm 0.003$ )
NSF67-60	4.5 ( $\pm 0.3$ )	4.3 ( $\pm 0.1$ )	5.6 ( $\pm 0.2$ )	4.0	4.1	5.3	1.02	1.29 (4.0d)	2.873 ( $\pm 0.102$ )
NSF80-20	4.3 ( $\pm 0.1$ )	2.0 ( $\pm 0.2$ )	2.3 ( $\pm 0.2$ )	4.1	1.7	2.0	0.41	1.17 (1.5d)	1.331 ( $\pm 0.109$ )
NSF80-40	4.5 ( $\pm 0.3$ )	3.5 ( $\pm 0.3$ )	4.8 ( $\pm 0.2$ )	4.0	3.0	4.5	0.75	1.50 (3.0e)	2.505 ( $\pm 0.104$ )
NSF80-60	5.3 ( $\pm 0.5$ )	5.8 ( $\pm 0.6$ )	8.1 ( $\pm 0.8$ )	4.5	4.8	6.8	1.06	1.41 (4.0e)	4.119 ( $\pm 0.380$ )
HSF64-20	3.5 ( $\pm 0.1$ )	2.1 ( $\pm 0.1$ )	2.6 ( $\pm 0.0$ )	3.3	2.0	2.5	0.60	1.25 (2.0d)	1.346 ( $\pm 0.021$ )
HSF64-40	3.8 ( $\pm 0.1$ )	3.0 ( $\pm 0.3$ )	4.3 ( $\pm 0.4$ )	3.6	2.5	3.7	0.69	1.48 (2.5e)	2.149 ( $\pm 0.183$ )
HSF64-60	5.0 ( $\pm 0.3$ )	3.9 ( $\pm 0.2$ )	5.7 ( $\pm 0.5$ )	4.5	3.6	4.9	0.80	1.36 (3.0e)	2.838 ( $\pm 0.208$ )
HSF67-20	3.8 ( $\pm 0.5$ )	1.9 ( $\pm 0.2$ )	2.0 ( $\pm 0.2$ )	2.9	1.5	1.7	0.51	1.13 (1.5d)	1.146 ( $\pm 0.050$ )
HSF67-40	3.9 ( $\pm 0.2$ )	2.7 ( $\pm 0.0$ )	4.4 ( $\pm 0.2$ )	3.6	2.7	4.1	0.75	1.66 (2.5e)	2.161 ( $\pm 0.056$ )
HSF67-60	4.2 ( $\pm 0.3$ )	4.5 ( $\pm 0.1$ )	7.2 ( $\pm 0.1$ )	3.7	4.3	7.0	1.16	1.62 (4.0e)	3.511 ( $\pm 0.051$ )
HSF80-20	4.3 ( $\pm 0.2$ )	1.9 ( $\pm 0.0$ )	2.8 ( $\pm 0.0$ )	4.0	1.9	2.8	0.47	1.47 (1.5e)	1.466 ( $\pm 0.009$ )
HSF80-40	4.5 ( $\pm 0.4$ )	3.8 ( $\pm 0.0$ )	5.4 ( $\pm 0.0$ )	3.8	3.8	5.3	1.00	1.39 (3.0e)	2.675 ( $\pm 0.080$ )
HSF80-60	5.5 ( $\pm 0.5$ )	6.1 ( $\pm 0.0$ )	8.1 ( $\pm 0.8$ )	4.7	6.1	6.8	1.29	1.11 (6.0d)	4.072 ( $\pm 0.227$ )

$f_L$ : flexural tensile strength corresponding to the limit of proportionality (LOP) or peak flexural tensile strength in the interval 0–0.05 mm of CMOD;  $f_{Ri}$ : residual flexural tensile strength corresponding to CMOD<sub>i</sub> (i=1, 2, 3, 4 mean the CMOD of 0.5, 1.5, 2.5 and 3.5 mm);  $f_{RiK}$ : the characteristic strength corresponding to  $f_{Ri}$ ;  $G_F$ : fracture energy defined by RILEM 50-FMC;  $\sigma$ : standard deviation

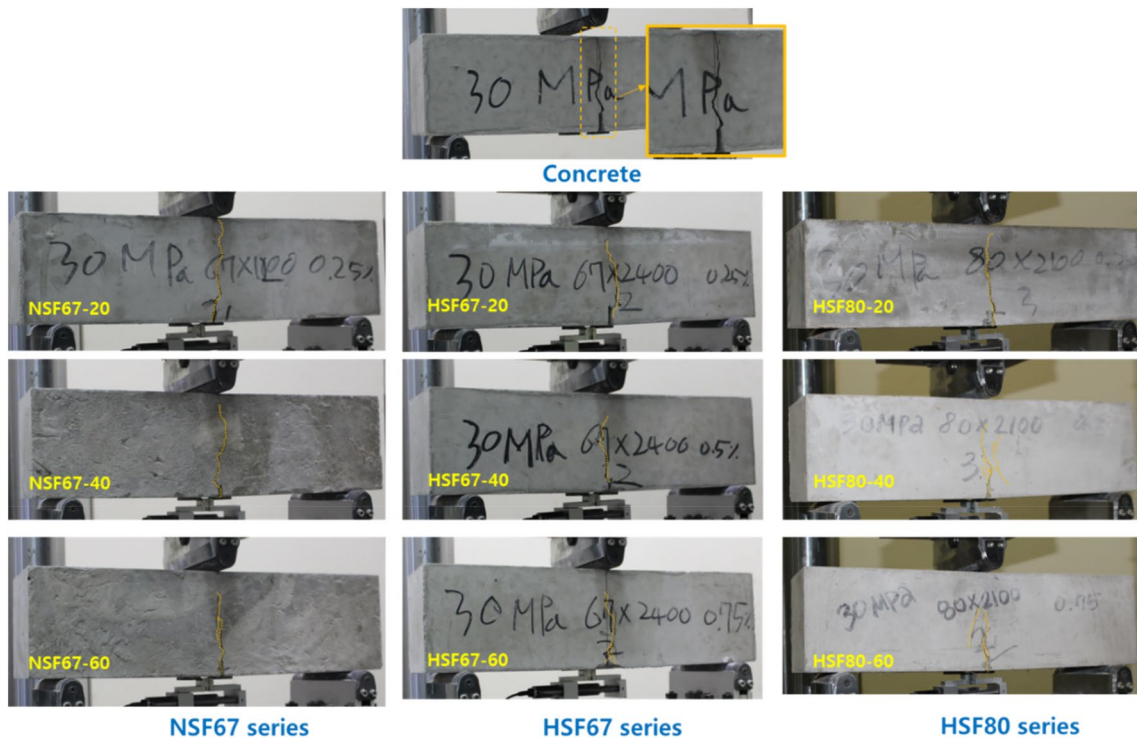


**Fig. 5** Typical failure patterns of SFRC notched specimens in bending

while in the SFRC specimen with lower  $l/d$  ratio, tensile strength and content of SFs, main crack almost propagates through the whole cross section of specimens at final failure. The finding on the failure patterns of SFRC specimens with different dosage and properties of SFs is consistent with the results in existing studies (Li et al., 2018; Liu et al., 2019) on the effects of fiber type, content and  $l/d$  ratio on the cracking patterns of PVA and steel fiber-reinforced concrete prisms in bending.

### 3.2.2 SFs' Properties Influence on Stress–CMOD Response

The flexural stress and CMOD curves of three SFRC notched prismatic specimens containing different fiber tensile strengths,  $l/d$  ratios and dosages were provided in Fig. 6. Each curve is an average flexural stress and CMOD relationship obtained from three specimens for each mixture. The flexural tensile strengths are also indicated on each curve in terms of the limit of proportionality ( $f_L$ ) and residual flexural tensile strengths ( $f_{R1}$ ,  $f_{R2}$ ,  $f_{R3}$ , and  $f_{R4}$  defined as the flexural strength corresponding to the specified CMOD of 0.5, 1.5, 2.5, and 3.5 mm, respectively). The curves indicate that the dosage and properties of hooked-end SFs have a significant effect on the flexural performance of SFRCs.

For SFRC mixtures with NSF64 and HSF64 SFs, the average flexural stress and CMOD curves of SFRC specimens show softening behavior irrespective of the dosage of SFs. The hooked-end SFs could increase the flexural stress up to CMOD of 3.5 mm without SF pull-out or breakage. From the zoomed-in curves in Fig. 6a, d, it can be seen that flexural stress increases with the increasing of CMOD and the initial slope of flexural stress and CMOD curve decreases slowly as CMOD increases before initial crack occurs. After the initial crack occurred, the flexural tensile stress decreased rapidly as the CMOD increased. The decrease in flexural tensile stress was more pronounced for SFRC specimens with lower tensile strength and smaller dosage of SFs. It is thought that the ability of SFRC to dissipate the fracture energy emitted during initial cracking process improves as the tensile strength and dosage of SFs increase. The flexural tensile stress gradually increased until the CMOD reached about 2.5 mm, and then remained constant until the CMOD of 3.5 mm and then gradually decreased. With adding SFs with  $l/d$  ratio of 64 into normal strength concrete, the flexural performance of SFRC was improved. There was no significant difference in the overall flexural behaviors of SFRC specimens reinforced with normal and high strength SFs. It is considered, because the normal and high strength SFs with lower  $l/d$  ratio were pulled out at crack surface, as shown in Fig. 7.

As shown in Fig. 6b, e, the overall flexural tensile stress and CMOD relationship curves of the SFRC specimen

with SFs having  $l/d$  ratio of 67 showed no significant difference from those of SFRC specimen reinforced with SFs with  $l/d$  ratio equal to 64. However, compared with NSF64-60 and HSF64-60 specimens, the flexural tensile stress less decreased in the NSF67-60 and HSF67-60 specimens after initial cracking. In particular, the SFRC specimen using the HSF67-60 mixture showed a flexural strain hardening response without flexural tensile stress degradation even after initial cracking. Both the NSF67-40 and HSF67-40 specimens showed a slight decrease in flexural tensile stress after initial cracking, but the HSF67-40 specimen showed flexural strain hardening behavior in which the flexural tensile stress increased as the CMOD increased. From Fig. 6e, it can be seen that high strength SFs with  $l/d$  ratio of 67 incorporated into normal strength concrete effectively bridge the cracks without reducing the flexural tensile stress until the CMOD reaches 4.0 mm. As a result of comparing the post-peak response of steel fiber reinforced concrete (SFRC), it was found that the behavior immediately after initial cracking did not show significant differences among specimens. However, the strain-hardening characteristics were more clearly observed in SFRC specimens reinforced with high-strength steel fibers. This is because the high tensile strength of the fibers allows them to perform an effective crack-bridging role even at larger crack widths resulting from crack progression. This is believed to result in less fiber pullout or fracture compared to normal strength SFs.

As described above, the overall flexural behavior of the NSF67-20 and HSF67-20 specimens did not show a significant difference, but for SFRC specimens with the SF dosage of more than 40 kg/m<sup>3</sup>, the flexural performance depended largely on the SF tensile strength.

The NSF80-60 and HSF80-60 specimens clearly showed flexural strain hardening behavior and no significant difference in flexural behavior. As shown in Fig. 7, normal strength SFs with higher  $l/d$  ratio in normal strength concrete bridge the crack surface until the fibers break, while high strength SFs with higher  $l/d$  ratio were pulled out, because the bonding strength between the SFs and the concrete matrix is relatively small compared to the tensile strength of the SFs. Regardless of the tensile strength and dosage of SFs, the SFRC specimen including NSF80 and HSF80 SFs showed a tendency to increase in flexural tensile stress until the CMOD reached from 2.5 mm to 3.0 mm. Then, as the CMOD increased, the flexural tensile stress decreased.

In conclusion, the content, tensile strength, and  $l/d$  ratio of SFs in normal-strength concrete have a significant effect on the flexural performance of SFRC, and it was found that the flexural performance of SFRC was sensitively affected by the amount and  $l/d$  ratio of SFs.

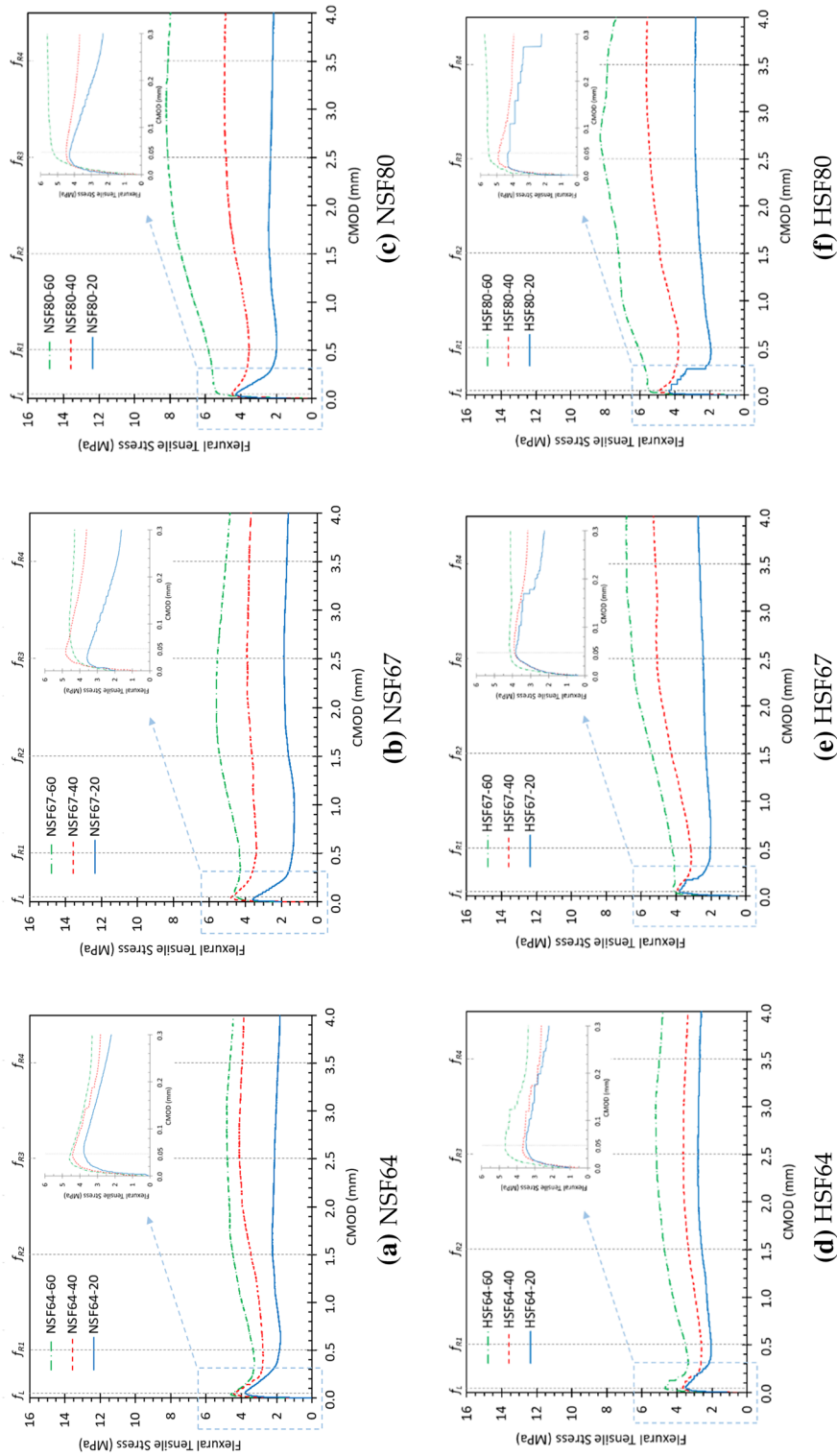


**Fig. 6** Average flexural tensile stress and CMOD relationship curves of SFRC notched specimens in bending

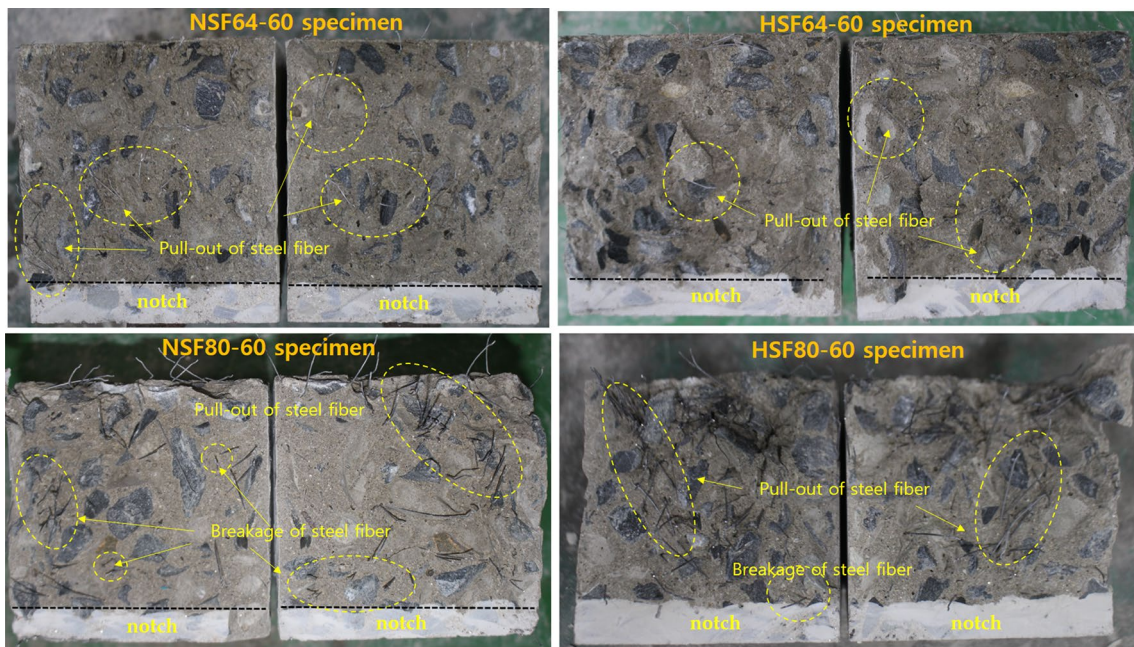


**Fig. 7** Broken section of SFRC notched beams in flexure

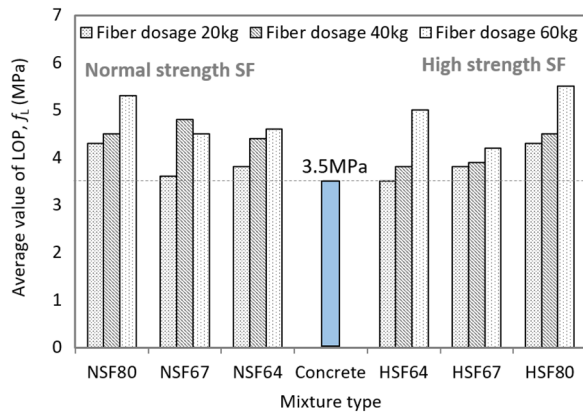


**Fig. 8** Average value of LOP ( $f_L$ ) of SFRC

### 3.2.3 SFs' Properties Influence on the Strength

Nominal values of SFRC properties can be evaluated from the flexural tensile stress and CMOD curves obtained by performing a three-point bending test on a notched beam according to EN 14652, as shown in Fig. 1a. These nominal values for SFRC mixtures investigated in the study are provided in Table 4 and Fig. 6.

**3.2.3.1 The Limit of Proportionality,  $f_L$**  The value of limit of proportionality (LOP)  $f_L$  is defined as the maximum flexural stress at the initial stage, i.e., CMOD value of less

or 0.05 mm. Average  $f_L$  of three specimens for each mixture illustrated in Fig. 8.

As shown in Table 4, the average  $f_L$  of all the SFRC mixtures was higher than that of concrete. As the dosage of NSF64 SFs increased from 20 to 60 kg/m<sup>3</sup>, the average  $f_L$  of the SFRC mixes increased by 8.5, 25.7, and 31.4% compared with that of concrete, respectively. In the SFRC specimens with the same amount of NSF67 SFs, the average  $f_L$  increased by 2.8, 37.1, and 28.6%, respectively. For SFRC mixes with NSF80 SFs, the average  $f_L$  was improved by 22.9, 28.6, and 51.5% compared with that of concrete, respectively. A similar trend was observed for SFRC mixtures using high strength SFs. As shown in Fig. 8, the maximum increase in average  $f_L$  of concrete reinforced with normal and high strength SFs was found in the NSF80-60 and HSF80-60 mixture, respectively. In particular, for the SFRC mixes with HSF80 SFs, an average  $f_L$  increased by 22.8, 28.6, and 57.1%, respectively, compared to concrete as the SF content increased from 20 to 60 kg/m<sup>3</sup>. Similar results were also reported by Chen et al. (Almusallam et al., 2016).

From the above results, it can be concluded that the higher  $l/d$  ratio and the larger content of hooked-end SFs, the more beneficial to average  $f_L$  of normal strength concrete.

**3.2.3.2 The Residual Flexural Tensile Strength,  $f_{Ri}$**  The MC2010 defines the parameters such as residual flexural tensile strength ( $f_{Ri}$ ) to describe the post-cracking

behavior of fiber-reinforced concrete (FRC). The residual flexural tensile strength is evaluated from flexural stress and CMOD relationship curve, as shown in Fig. 6. Average residual flexural tensile strength in the flexural tensile stress and CMOD relationship curves for each SFRC mixture is included in Fig. 6. In addition, the residual flexural tensile strengths ( $f_{R1}$  and  $f_{R3}$ ) at the serviceability limit state (SLS) and ultimate limit state (ULS) are summarized in Table 4.

Fig. 9 shows the variation in the average residual flexural tensile strength of three SFRC beam specimens with different amount, tensile strength and  $l/d$  ratio of SFs. As shown in Fig. 9a and Table 4, the residual flexural strength ( $f_{R1}$ ) at SLS (CMOD=0.5 mm) for NSF65-20, NSF67-20, and NSF80-20 specimens are 1.8, 1.4, and 2.0 MPa, respectively. At ULS (CMOD=2.5 mm), the maximum and minimum residual flexural strengths ( $f_{R3}$ ) are 1.9 MPa in NSF64-20 and 2.3 MPa in NSF80-20, respectively. The post-cracking behavior of SFRC specimens with SF amount of 20 kg/m<sup>3</sup> can be characterized by maintaining the residual flexural tensile strength at SLS until the CMOD reached 4.0 mm. The post-cracking behavior in the SFRC specimens with SF contents of 40 and 60 kg/m<sup>3</sup> can be characterized by strain-hardening behavior in which the residual flexural strength gradually increases as the CMOD increases to 4.0 mm. These characteristics became more pronounced as the  $l/d$  ratio of SFs increased.

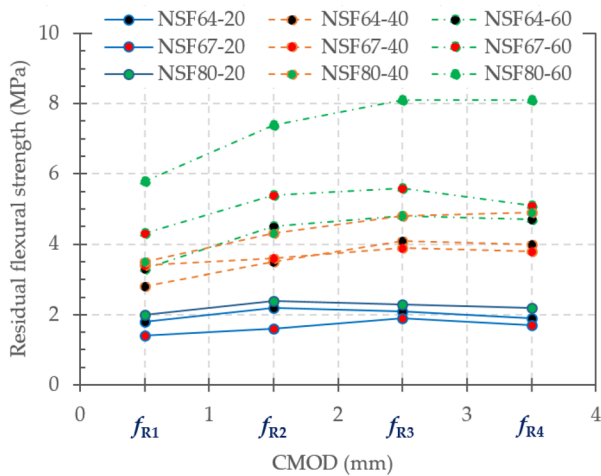
Fig. 9b shows that  $f_{R1}$  for HSF65-20, HSF67-20, and HSF80-20 specimens are 2.0, 1.9, and 1.90 MPa, respectively. The  $f_{R3}$  for HSF65-20, HSF67-20, and HSF80-20 specimens was 24, 10, and 45% larger than  $f_{R1}$ , respectively. Unlike the SFRC specimens with normal strength

SFs, SFRC specimens with lower amount (20 kg/m<sup>3</sup>) of high strength SFs clearly exhibited strain hardening properties as post-cracking behaviors.

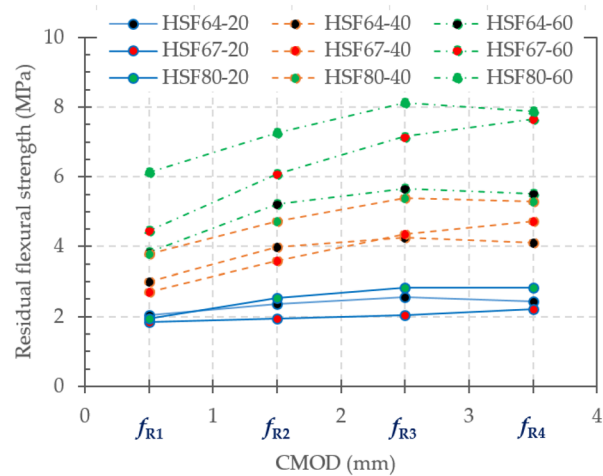
From the experimental results analysis on the residual flexural tensile strength ( $f_{Rj}$ ) of SFRC mixed in the study, it can be concluded that the post-flexural cracking behavior of SFRC improves as the tensile strength, the  $l/d$  ratio, and the dosage of hooked-end SFs increases, because higher strength, dosage and  $l/d$  ratio of SFs result in a stronger bridging effect across the crack surface. This result is in agreement with the results reported in the existing studies by Venkateshwaran et al., 2018 and Chen et al., 2021.

To classify the post-cracking strength of FRC, the MC2010 also defines the characteristic strength, denoted by  $f_{Rjk}$ , as the strength value of each group below which no more than 5% of the test results may be expected to fall in. The classification is based on two post-cracking residual strengths ( $f_{R1k}$  and  $f_{R3k}$ ) at CMOD=0.5 mm and CMOD=2.5 mm, which characterize the material behavior at SLS and at ULS, respectively (fib Bulletin 65/66: Model Code 2010, 2012; Prisco et al., 2013). An FRC material can be classified using a couple of parameters: the first one is a number denoting the  $f_{R1k}$  class, the second is a letter denoting the ratio of  $f_{R3k}/f_{R1k}$ . More information can be obtained from MC2010.

For each SFRC mixture considered in the study, parameters required for the classification according to MC2010 are illustrated in Fig. 10. As shown in Fig. 10a, the characteristic flexural strength ( $f_{R1k}$ ) of NSF64-20, NSF67-20, and NSF80-20 mixtures at SLS is 1.1, 1.2, and 1.4 MPa, respectively. The  $f_{R1k}$  of HSF64-20, HSF67-20, and HSF80-20 mixes ranges from 1.5 to 2.0 MPa according to

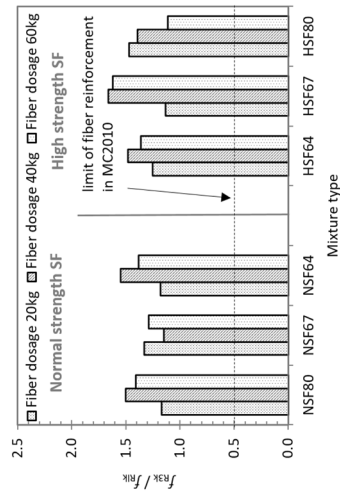


(a) SFRC with normal strength SF (NSF)

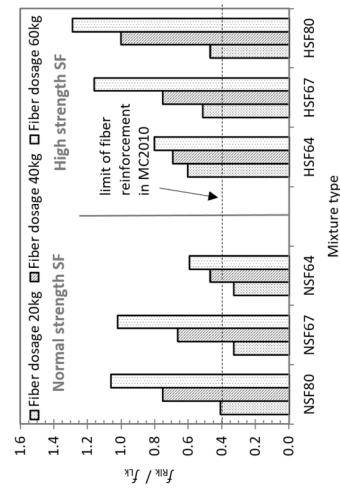


(b) SFRC with high strength SF (HSF)

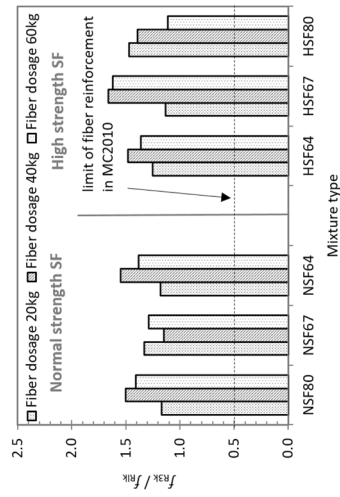
Fig. 9 Average residual flexural tensile strength ( $f_{Rj}$ ) of SFRC specimens



(a) Characteristic strength  $f_{Rk}$



(b)  $f_{Rk} / f_{Lk}$



(c)  $f_{R3k} / f_{R1k}$

**Fig. 10** Characteristic residual flexural tensile strength of SFRC specimens

$l/d$  ratio of SFs. Compared to SFRC mixtures with normal strength SFs, SFRC specimens including high strength SFs showed 1.1–1.8 times higher characteristic flexural strength ( $f_{R1k}$ ) at SLS. In SFRC specimens with SF dosages of 40 and 60  $\text{kg/m}^3$ , the  $f_{R1k}$  increases as the tensile strength and content of SFs increase.

Since plain concrete subjected to tensile force exhibits brittle failure pattern, brittle failure must be prevented of concrete structural members. Therefore, reinforcement such as reinforcing bars or welded mesh must be properly placed for bearing the tensile stress applied to the structural members. The MC2010 permits the full or partial replacement of conventional reinforcement with fiber reinforcement at ULS. The following relationships are suggested as the acceptance criteria:

$$\frac{f_{R1k}}{f_{Lk}} > 0.4 \tag{1}$$

$$\frac{f_{R3k}}{f_{R1k}} > 0.5 \tag{2}$$

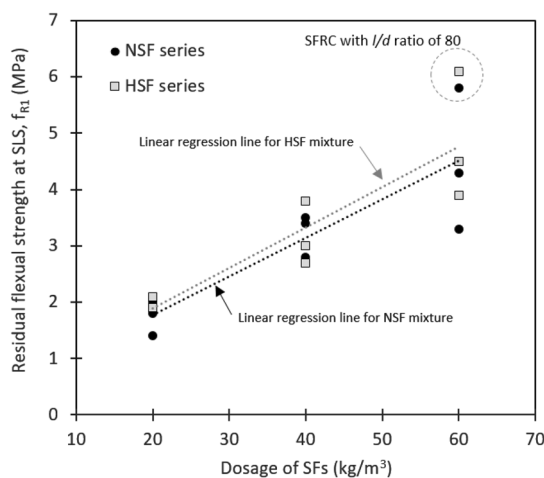
$f_{R1k}/f_{Lk}$  and  $f_{R3k}/f_{R1k}$  for all the SFRC mixtures are provided in Fig. 10b, c. The  $f_{R1k}/f_{Lk}$  ratio of both NSF64-20 and NSF67-20 mixtures was the same as 0.33. Except for these mixtures, the first criterion was satisfied in all SFRC mixtures. The  $f_{R3k}/f_{R1k}$  ratio of all the SFRC mixtures was more than 0.5 and the second criterion was fulfilled in all the SFRCs mixed in the study.

Therefore, with the exception of the both SFRC mixtures with 20  $\text{kg/m}^3$  of normal strength SFs having  $l/d$  ratio of 64 and 67 (NSF64-20 and NSF67-20), it was confirmed that all SFRC mixtures considered in this study

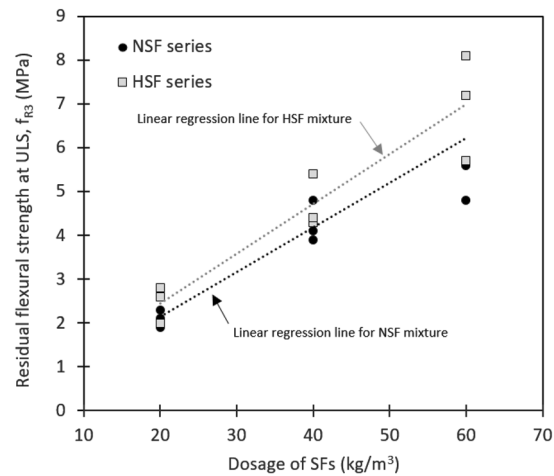
could be substituted with a part of the reinforcing bars which resist the applied tensile stress to the structural member.

At using FRC for structural members, MC 2010 stipulates that the designer should specify the residual flexural strength class as well as the material of the fiber. As shown in Table 4 and Fig. 10, the classification defined by MC2010 varied from 1.0c to 4.0e for SFRC mixtures with normal strength SFs, while for SFRC mixtures incorporating high strength SFs, their classes varied from 2.0d to 6.0d. Chen et al., 2021 reported that for SFRC with normal strength SF dosage of 20  $\text{kg/m}^3$  and compressive strength ranging from 31 to 36 MPa, the classification of SFRC reinforced with hooked-end SF aspect ratio of 65, 80, and 100 was 1c, 1.5d, and 1.5c, respectively. Similar tendencies were also found by Mudadu et al., 2018.

Fig. 11 shows the variation of residual flexural tensile strength  $f_{R1}$  at SLS and  $f_{R3}$  at ULS according to dosages of normal and high strength SFs. Based on the experimental results, a linear regression line was derived and included in Fig. 11. Regardless of the tensile strength of the SFs,  $f_{R1}$  and  $f_{R3}$  tend to increase as the dosages of SFs increases. At the same content of SFs,  $f_{R1}$  and  $f_{R3}$  of SFRC mixtures with high strength SFs were higher than those of normal strength SFs. This trend was more pronounced in  $f_{R3}$  than in  $f_{R1}$ . When the tensile strength of fibers that cross a crack is high, their ability to resist being pulled-out or broken is improved compared to when their tensile strength is low. Therefore, this leads to an increase in the crack bridging performance of steel fibers as cracks propagate, resulting in increased toughness. This finding is consistent with other research (Choi et al., 2019). As the dosage of SFs increased from 40 to 60, the residual



(a) Residual flexural strength at SLS,  $f_{R1}$



(b) Residual flexural strength at ULS,  $f_{R3}$

**Fig. 11** Residual flexural tensile strength of concrete beams with different strength of SFs

flexural strength at SLS showed a proportional increase, as shown in Fig. 11a. In particular, the effect of the dosage of SFs on residual flexural strength at SLS became more significant as the  $l/d$  ratio of SF increased. This is because, under the same dosage conditions, a higher  $l/d$  ratio of SF results in a lower number of fibers, leading to a higher probability of individual fibers being arranged in a separate manner, which is believed to be effective in crack control. Based on these results, it can be concluded that even of a smaller dosage of high strength SFs is added, the residual flexural tensile strength comparable to that of SFRC mixture with normal strength SFs can be obtained.

**3.2.3.3 The Fracture Energy,  $G_f$**  To evaluate the fracture energy for each SFRC mix used in this experimental program, the area under the load and CMOD curve for notched beam specimen was calculated up to the specified CMOD of 4 mm. Hillerborg work-of-fracture method, which is adopted by the RILEM TC 50-FMC (Hillerborg, 1983), was used to calculate the fracture energy. The mean value of the fracture energy for three specimens of each SFRC mix is given in Table 4 and the mean value of fracture energy is plotted in Fig. 12.

As can be observed from Fig. 12, the dosage,  $l/d$  ratio, and tensile strength of hooked-end SFs have a significant effect on the flexural fracture energy absorption capacity of SFRC beam specimens. For SFRC mix with normal strength SFs, the fracture energy of NSF64-20, NSF67-20, and NSF80-20 mixes is 1.21, 0.99, and 1.33  $\text{kJ/m}^2$ , respectively. The amount of energy absorbed by NSF67-20 is the least, while the fracture energy of NSF80-20 is the largest. In addition, a similar trend is shown in the SFRC with high strength SF content of 20  $\text{kg/m}^3$ . However, for SFRC mixes with SF dosages of 40 and 60  $\text{kg/m}^3$ , the fracture energy clearly increases as  $l/d$  ratio and dosage of SFs increase. The fracture

energy of HSF64-60 and HSF67-80 is 1.15 and 1.22 times higher than those of NSF64-60 and NSF67-60, while the energy absorbed by HSF80-60 is comparable to that by NSF80-60. The fracture energy of HSF64-40 and HSF80-40 is 1.04 and 1.07 times higher than those of NSF64-40 and NSF80-40, while the fracture energy of HSF67-40 is similar to that of NSF67-40. As a result, it can be concluded that the fracture energy of SFRC is more sensitive for the dosage of SFs than for the tensile strength of SFs.

#### 4 Conclusions

This study concerns the mechanical properties, such as compressive and flexural behavior, of normal strength concrete reinforced with different  $l/d$  ratio, tensile strength and dosage of hooked-end SFs. Based on results achieved the following conclusion can be stated:

1. The compressive toughness, Poisson's ratio ( $\nu$ ) and strain ( $\epsilon_{co}$ ) at compressive strength increased with the increase of the SFs content, while the increase of compressive strength and elastic modulus were not significant. The tensile strength and  $l/d$  of SFs had little effect on the compressive properties of SFRC.
2. Higher tensile strength, higher content and larger  $l/d$  ratio of SFs have a positive effect on the improvement in the flexural response of SFRC, while the normal strength concrete with SF dosage exhibits a combination of both flexural strain softening and hardening behavior, HSF67-60, and HSF80-60 SFRC mixes show a distinct strain hardening behavior.
3. The limit of proportionality (LOP),  $f_L$  of SFRC is higher by 8–57% than that of conventional concrete. The  $f_L$  increased with increasing with the dosage of SFs. The enhancement of  $f_L$  in the SFRC mix remarkable as  $l/d$  ratio of SFs increases.
4. To substitute partially conventional reinforcement for preventing the brittle failure of structural members as stipulated in MC2010, it is recommended that the dosage of normal strength SFs with  $l/d$  ratios of 64 and 67 is less than 30  $\text{kg/m}^3$ , while the dosage of SFs with  $l/d$  ratio of more than 67 could be reduced up to 20  $\text{kg/m}^3$ . For high strength SFs, a minimal content of 20  $\text{kg/m}^3$  is recommended.
5. In normal strength concrete, the fracture energy showed little difference according to the tensile strength of SFs. However, an increase in the dosage and  $l/d$  ratio of SFs had a positive effect on the fracture energy ( $G_f$ ).

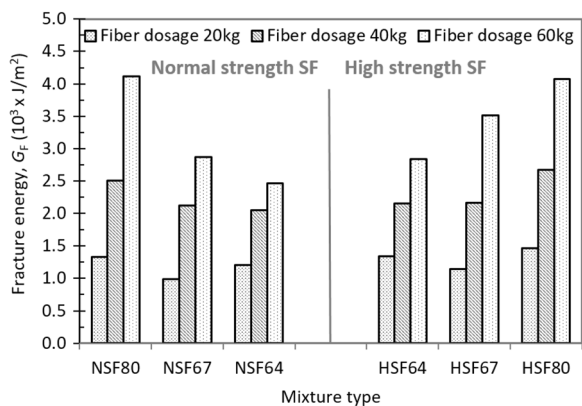


**Fig. 12** Fracture energy of SFRC

**Acknowledgements**

This work is supported by the National Research Foundation of Korea (NRF-2016R1D1A3B02008179).

**Author contributions**

S-JJ who planned the test and wrote mainly the paper; D-HK, QW, W-JJ and A-HJ who performed tests and organized the test results; W-SP and S-WK analyzed the test results and reviewed the written paper; H-DY is a PI of the research project and proposed the idea of the research. All authors read and approved the final manuscript.

**Funding**

National Research Foundation of Korea (NRF-2016R1D1A3B02008179).

**Availability of data and materials**

Not applicable.

**Declarations****Ethics approval and consent to participate**

Not applicable.

**Consent for publication**

Not applicable.

**Competing interests**

The authors declare that they have no competing interests.

Received: 7 December 2022 Accepted: 3 May 2023

Published online: 24 August 2023

**References**

- Abadel, A., Abbas, H., Almusallam, T., Al-Salloum, Y. A., & Siddiqui, N. (2016). Experimental and analytical investigations of mechanical properties of hybrid fiber reinforced concrete. *Magazine of Concrete Research*, 68(16), 823–843.
- Abbass, W., Khan, M. I., & Mourad, S. (2018). Evaluation of mechanical properties of steel fiber reinforced concrete with different strengths of concrete. *Construction and Building Materials*, 168, 556–569.
- ACI Committee 318. (2008) Building code and commentary, Report ACI 318-08/318R-08. American Concrete Institute, Farmington Hills, MI
- ACI Committee 544. (2009). State-of-the-Art Report on Fiber Reinforced Concrete, Report ACI 544.1R. American Concrete Institute. Farmington Hills, MI
- Almusallam, T., Ibrahim, S. M., Al-Salloum, Y., Abadel, A., & Abbas, H. (2016). Analytical and experimental investigations on the fracture behavior of hybrid fiber reinforced concrete. *Cement and Concrete Composites*, 74, 201–217.
- Balaguru, P., & Ramakrishnan, V. J. M. J. (1988). Properties of fiber reinforced concrete: Workability, behavior under long-term loading, and air-void characteristics. *ACI Materials Journal*, 85(3), 189–196.
- Bhogone, M. V., & Subramaniam, K. V. (2021). Early-age tensile constitutive relationships for steel and polypropylene fiber reinforced concrete. *Engineering Fracture Mechanics*, 244, 107556.
- Chen, G., Gao, D., Zhu, H., Yuan, J. S., Xiao, X., & Wang, W. (2021). Effects of novel multiple hooked-end steel fibres on flexural tensile behaviour of notched concrete beams with various strength grades. *Structures*, 33, 3644–3654.
- Chen, G., Zhao, L., Gao, D., Yuan, J., Bai, J., & Wang, W. (2022). Flexural Tensile Behavior of Single and Novel Multiple Hooked-End Steel Fiber-Reinforced Notched Concrete Beams. *Journal of Materials in Civil Engineering*, 34(6), 04022077.
- Choi, W. C., Jung, K. Y., Jang, S. J., & Yun, H. D. (2019). The influence of steel fiber tensile strengths and aspect ratios on the fracture properties of high-strength concrete. *Materials*, 12(13), 2105.
- Deifalla, A. F., Zapris, A. G., & Chalioris, C. E. (2021). Multivariable regression strength model for steel fiber-reinforced concrete beams under torsion. *Materials*, 14(14), 3889.
- Di Prisco, M., Colombo, M., & Dozio, D. (2013). Fibre-reinforced concrete in fib Model Code 2010: Principles, models and test validation. *Structural Concrete*, 14(4), 342–361.
- Ding, Y., & Kusterle, W. (2000). Compressive stress–strain relationship of steel fibre-reinforced concrete at early age. *Cement and Concrete Research*, 30(10), 1573–1579.
- EN 12350-1. (2009). Testing Fresh Concrete—Part 1: Sampling and common apparatus. *European Committee for Standardization*, Brussels
- EN 14651. (2005). Test Method for Metallic Fibre Concrete—Measuring the Flexural Tensile Strength (Limit of Proportionally (LOP), Residual). *European Committee for Standardization*, Brussels. 18
- fib Bulletin 65/66: Model Code 2010. (2012). International Federation for structural concrete (fib). Lausanne, Switzerland
- Gao, D., & Wang, F. (2021). Effects of recycled fine aggregate and steel fiber on compressive and splitting tensile properties of concrete. *Journal of Building Engineering*, 44, 102631.
- Guler, S., & Akbulut, Z. F. (2022). Residual strength and toughness properties of 3D, 4D and 5D steel fiber-reinforced concrete exposed to high temperatures. *Construction and Building Materials*, 327, 126945.
- Hillerborg, A. R. N. E. Concrete fracture energy tests performed by 9 laboratories according to a draft RILEM recommendation. *Report to RILEM TC50-FMC, Report TVBM-3015, 1983, Lund, Sweden.*
- Johnston, C. D. (1984). Measures of the workability of steel fiber reinforced concrete and their precision. *Cement, Concrete and Aggregates*, 6(2), 74–83.
- JSCE-SF5. (1984). Method of tests for compressive strength and compressive toughness of steel fiber reinforced concrete." *Concrete library of JSCE.* Japan Society of Civil Engineers (JSCE), Tokyo, Japan
- Kachouh, N., El-Maaddawy, T., El-Hassan, H., & El-Ariss, B. (2022). Shear response of recycled aggregates concrete deep beams containing steel fibers and web openings. *Sustainability*, 14(2), 945.
- Korean standard. (2017). Standard Test Method for Compressive Strength of Concrete, KS F 2405. (<https://standard.go.kr/KSCI/>) in Korean
- Kytinou, V. K., Chalioris, C. E., & Karayannis, C. G. (2020). Analysis of residual flexural stiffness of steel fiber-reinforced concrete beams with steel reinforcement. *Materials*, 13(12), 2698.
- Lantsoght, E. O. (2019). How do steel fibers improve the shear capacity of reinforced concrete beams without stirrups? *Composites Part B: Engineering*, 175, 107079.
- Lee, S. C., Oh, J. H., & Cho, J. Y. (2015). Compressive behavior of fiber-reinforced concrete with end-hooked steel fibers. *Materials*, 8(4), 1442–1458.
- Li, B., Chi, Y., Xu, L., Shi, Y., & Li, C. (2018). Experimental investigation on the flexural behavior of steel-polypropylene hybrid fiber reinforced concrete. *Construction and Building Materials*, 191, 80–94.
- Li, B., Xu, L., Chi, Y., Huang, B., & Li, C. (2017). Experimental investigation on the stress-strain behavior of steel fiber reinforced concrete subjected to uniaxial cyclic compression. *Construction and Building Materials*, 140, 109–118.
- Li, C., Shang, P., Li, F., Feng, M., & Zhao, S. (2020). Shrinkage and mechanical properties of self-compacting SFRC with calcium-sulfoaluminate expansive agent. *Materials*, 13(3), 588.
- Liu, F., Ding, W., & Qiao, Y. (2019). Experimental investigation on the flexural behavior of hybrid steel-PVA fiber reinforced concrete containing fly ash and slag powder. *Construction and Building Materials*, 228, 116706.
- Marcos-Meson, V., Michel, A., Solgaard, A., Fischer, G., Edvardsen, C., & Skovhus, T. L. (2018). Corrosion resistance of steel fibre reinforced concrete—A literature review. *Cement and Concrete Research*, 103, 1–20.
- Mertol, H. C., Baran, E., & Bello, H. J. (2015). Flexural behavior of lightly and heavily reinforced steel fiber concrete beams. *Construction and Building Materials*, 98, 185–193.
- Mudadu, A., Tiberti, G., Germano, F., Plizzari, G. A., & Morbi, A. (2018). The effect of fiber orientation on the post-cracking behavior of steel fiber reinforced concrete under bending and uniaxial tensile tests. *Cement and Concrete Composites*, 93, 274–288.
- Pakravan, H. R., Latifi, M., & Jamshidi, M. (2017). Hybrid short fiber reinforcement system in concrete: A review. *Construction and Building Materials*, 142, 280–294.
- Romualdi, J. P., & Batson, G. B. (1963). Mechanics of crack arrest in concrete. *Journal of the Engineering Mechanics Division*, 89(3), 147–168.

- Serna, P., Arango, S., Ribeiro, T., Núñez, A. M., & Garcia-Taengua, E. (2009). Structural cast-in-place SFRC: Technology, control criteria and recent applications in Spain. *Materials and Structures*, 42(9), 1233–1246.
- Shoab, A., & Lubell, A. S. (2021). Effect of mix composition on the mechanical properties of SFRC. *Construction and Building Materials*, 286, 122760.
- Soufeiani, L., Raman, S. N., Jumaat, M. Z. B., Alengaram, U. J., Ghadyani, G., & Mendis, P. (2016). Influences of the volume fraction and shape of steel fibers on fiber-reinforced concrete subjected to dynamic loading—A review. *Engineering Structures*, 124, 405–417.
- The Concrete Society. (2007). Guidance for the design of steel-fibre-reinforced concrete. Camberley, Surrey, UK
- Venkateshwaran, A., Tan, K. H., & Li, Y. (2018). Residual flexural strengths of steel fiber reinforced concrete with multiple hooked-end fibers. *Structural Concrete*, 19(2), 352–365.
- Voutetaki, M. E., Naoum, M. C., Papadopoulos, N. A., & Chalioris, C. E. (2022). Cracking diagnosis in fiber-reinforced concrete with synthetic fibers using piezoelectric transducers. *Fibers*, 10(1), 5.
- Wang, X., Fan, F., Lai, J., & Xie, Y. (2021). Steel fiber reinforced concrete: A review of its material properties and usage in tunnel lining. *Structures*, 34, 1080–1098.
- Yazıcı, Ş., Inan, G., & Tabak, V. (2007). Effect of aspect ratio and volume fraction of steel fiber on the mechanical properties of SFRC. *Construction and Building Materials*, 21(6), 1250–1253.
- Zhang, P., Kang, L., Wang, J., Guo, J., Hu, S., & Ling, Y. (2020). Mechanical properties and explosive spalling behavior of steel-fiber-reinforced concrete exposed to high temperature—a review. *Applied Sciences*, 10(7), 2324.
- Zollo, R. F. (1997). Fiber-reinforced concrete: An overview after 30 years of development. *Cement and Concrete Composites*, 19(2), 107–122.

### Publisher's Note

Springer Nature remains neutral with regard to jurisdictional claims in published maps and institutional affiliations.

**Seok-Joon Jang** Deputy department head, PhD, Building Management Support Center, Korea Authority of Land & Infrastructure, Jinju-si, Gyeongsangnam-do, 52856, Republic of Korea.

**Wan-Shin Park** Professor, PhD, Department of construction engineering education, Chungnam National University, Yuseong-gu, Daejeon, 34134, Republic of Korea.

**Sun-Woo Kim** Professor, PhD, Department of construction engineering education, Chungnam National University, Yuseong-gu, Daejeon, 34134, Republic of Korea.

**Dong-Hui Kim** graduate student, Department of Architectural engineering, Chungnam National University, Yuseong-gu, Daejeon, 34134, Republic of Korea.

**Qi Wang** graduate student, Department of Architectural engineering, Chungnam National University, Yuseong-gu, Daejeon, 34134, Republic of Korea.

**Woo-Jin Jeong** graduate student, Department of Architectural engineering, Chungnam National University, Yuseong-gu, Daejeon, 34134, Republic of Korea.

**Ai-Hua Jin** graduate student, Department of Architectural engineering, Chungnam National University, Yuseong-gu, Daejeon, 34134, Republic of Korea.

**Hyun-Do Yun** Professor, PhD, Department of Architectural engineering, Chungnam National University, Yuseong-gu, Daejeon, 34134, Republic of Korea.

Submit your manuscript to a SpringerOpen<sup>®</sup> journal and benefit from:

- Convenient online submission
- Rigorous peer review
- Open access: articles freely available online
- High visibility within the field
- Retaining the copyright to your article

---

Submit your next manuscript at ► [springeropen.com](https://www.springeropen.com)

---